Defence Technology 13 (2017) 72–76

Contents lists available at ScienceDirect

Defence Technology

journal homepage: www.elsevier.com/locate/dt

A novel method to fabricate TiAl intermetallic alloy 3D parts using additive manufacturing

J.J.S. Dilip [a, *], H. Miyanaji [a], Austin Lassell [a], Thomas L. Starr [b], Brent Stucker [c]

[a] Rapid Prototyping Center, Department of Industrial Engineering, University of Louisville, Louisville, KY 40292, USA
[b] Department of Chemical Engineering, University of Louisville, Louisville, KY 40292, USA
[c] 3DSIM, 1794 Olympic Parkway, Suite 110, Park City, UT 84098, USA

ARTICLE INFO

Article history:
Received 24 May 2016
Accepted 23 August 2016
Available online 3 September 2016

Keywords:
Additive manufacturing
Binder jetting
Intermetallic
Titanium aluminide
Reactive sintering

ABSTRACT

The present work explores the feasibility of fabricating porous 3D parts in TiAl intermetallic alloy directly from Ti–6Al–4V and Al powders. This approach uses a binder jetting additive manufacturing process followed by reactive sintering. The results demonstrate that the present approach is successful for realizing parts in TiAl intermetallic alloy.

1. Introduction

Titanium-aluminides (TiAl) have low density (3.9 g/cm^3), good high temperature strength and superior resistance to oxidation (above 750 °C) giving them the potential to be used as light weight and high-temperature structural materials [1,2]. As such, these properties make the material quite attractive for aerospace and automobile applications. Recently, porous TiAl alloys are also being considered for high temperature liquid and gas separation filters [3]. TiAl alloys of technical significance have the general composition of Ti–Al (42–49) -X (0.1–1.0), where X represents alloying elements such as Cr, Nb, W, V, Ta, Si, B, and C [2,4]. Currently, large scale processing methods such as ingot casting, powder processing and ingot forging, sheet production by hot-rolling, powder metallurgy processing, investment casting and permanent mold casting are used to fabricate TiAl. However, these conventional methods pose significant challenges in processing of the alloy leading to higher production costs [1,2]. Given the ordered tetragonal structure and strong bonding between Ti and Al, the alloy is inherently brittle, making machining and shaping difficult [1]. To overcome such problems net-shape fabrication technologies such as powder metallurgy have been considered [2].

Additive manufacturing (AM) is advantageous for a number of reasons, including extensive design freedom in terms of geometry. Recent work have focused on the use of selective laser melting and electron beam melting AM processes to fabricate TiAl parts [5,6]. However, these processes encounter problems because they inherently involve melting and solidification stages. Also these processes suffer a variety of metallurgical problems such as solid state cracking due to thermal stresses from the inherent brittleness of as-cast TiAl microstructures [5–7]. In contrast, binder jetting avoids these problems as it is a low temperature process. In binder jetting powder is deposited layer by layer and binder is applied in the regions of interest, creating a green part directly from a CAD model. Subsequently, the green part from the printer is oven cured and sintered [7,8].

This study evaluates the feasibility of fabricating titanium aluminide (TiAl) parts by using Ti–6Al–4V and Al powders via binder jetting followed by a reactive sintering treatment. This route to produce TiAl intermetallic alloy parts can be economical when compared to the use of TiAl powders since TiAl powder is very expensive.

2. Materials and methods

In the present study two metal powders were used; atomized Al (Pyrochem, USA) and Ti–6Al–4V (Raymor-Grade 23) powders with

* Corresponding author.
E-mail address: samueldilip@gmail.com (J.J.S. Dilip).
Peer review under responsibility of China Ordnance Society.

http://dx.doi.org/10.1016/j.dt.2016.08.001

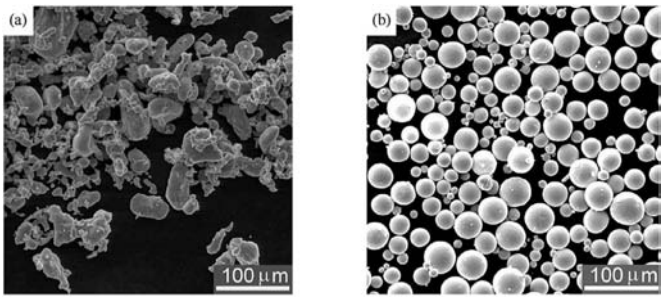

Fig. 1. SEM micrographs showing morphology of (a) Al powder and (b) Ti–6Al–4V powder used.

average particle size near 30 μm and 45 μm respectively. The powders were mixed in equi-atomic proportion (by Wt %) Al to achieve TiAl after sintering. The ExOne binder jetting printer was used to build 3D parts of 10 × 10 × 3 mm in size. The parameters used during binder jetting are as follows: 100 μm layer thickness, 60% binder drying power, 45 s dry time, jet feed rate 2 mm/min and 60% binder saturation level. The binder used for the experiment was "ExOne PM-B-SR1-04", an ether solvent based binder. The green parts from the printer were carefully loaded into an oven to cure the binder at 200 °C for 2 h. The cured parts were then subjected to reactive sintering at temperatures of 600 °C and 800 °C for 6 h, as well as 1000 °C for 6 h and 24 h in nitrogen atmosphere. Microstructural characterization of the powders and sintered parts was carried out using SEM equipped with EDS. Phase analysis of the steel powder and as-built samples were characterized using X-Ray Diffraction with Cu–Kα radiation ($\lambda = 1.54$ A°). The phases formed were identified by comparison of the recorded diffraction peaks with the ICDD database. Density of the sintered parts was measured using the Archimedes method according to ASTM B962-08.

3. Results and discussion

The size and morphology of the powders can be observed from the SEM micrographs presented in Fig. 1. The Al powder particles (Fig. 1(a)) are irregular in shape, whereas the Ti–6Al–4V alloy powder particles (Fig. 1(b)) are spherical in shape in a bimodal distribution.

Fig. 2(a) shows the samples sintered at different temperatures. The samples sintered at 600 °C appear bright (gray), whereas the samples sintered at higher temperatures appear black. This change in luster is attributed to the reaction products formed during sintering. The surface morphology of the sample sintered at 600 °C is presented in Fig. 2(b). The micrograph shows predominantly unreacted Al (irregular) and Ti–6Al–4V (spherical) particles. On any given Ti–6Al–4V particle, conical structures can be seen growing on the surface and interconnecting neighboring Ti–6Al–4V particles together. EDS analysis indicates these interconnecting channels have the composition of $TiAl_3$. Fig. 2(c) shows the surface morphology of a sample sintered at 800 °C for 6 h. Clearly, the surfaces of the particles appear different (grainier) than those sintered at 600 °C. The in-set in Fig. 2(c) shows a high magnification micrograph revealing the surface texture. Given the sintering

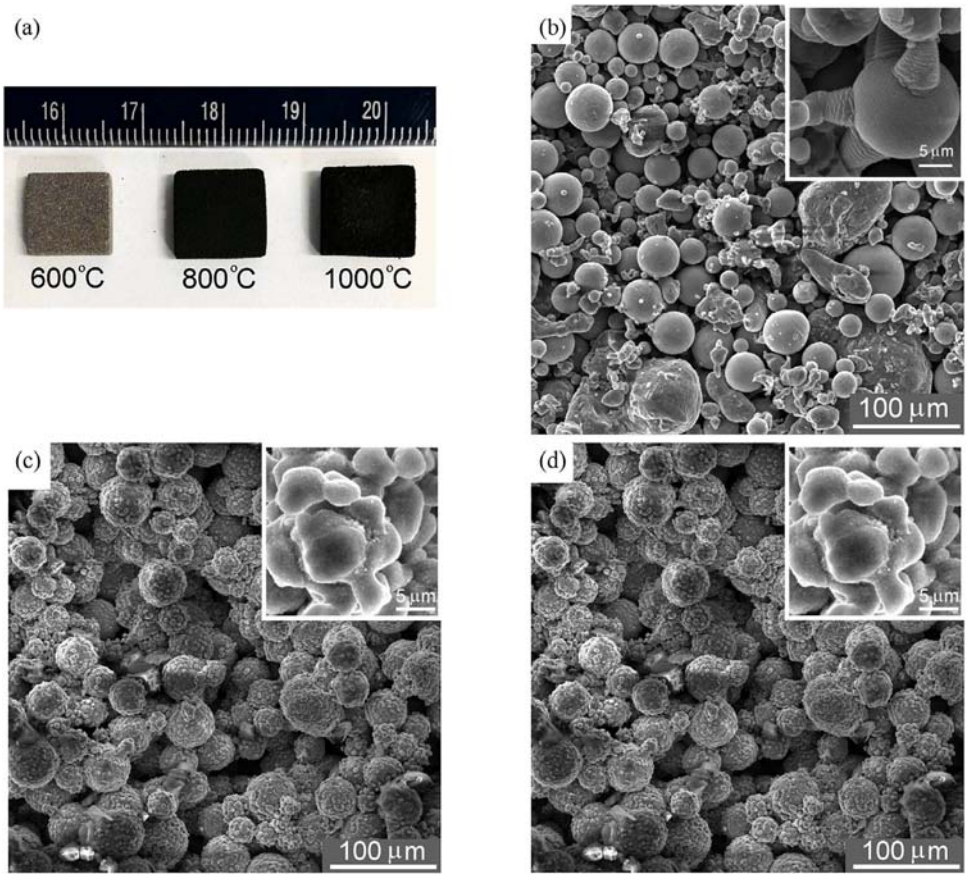

Fig. 2. (a) Photograph of sintered samples. SEM micrographs showing surface morphology of samples sintered for 6 h at 600 °C (b), 800 °C (c) and 1000 °C (d). High magnification micrographs are shown in the in-sets.

temperature was above the melting temperature of Al, liquid phase sintering occurs. The Ti–6Al–4V particles retain the original spherical morphology and the surface contains reaction product. EDS analysis on the surface confirms the presence of $TiAl_3$. Initially, Ti atoms on the surface will dissolve in liquid Al and the Ti enriched solution will recast onto the sintered particles, resulting in $TiAl_3$. The appearance of small globular features (due to surface tension) on the sintered particle surfaces indicate recasting has occurred.

At the melting temperature of Al, the diffusion of Al in Ti is 75×10^{-3} mm/s while the diffusion of Ti in the Al is 66×10^{-3} mm/s [3]. Given the higher diffusion of Al atoms into Ti particles the result is the enrichment of Al, which aids in forming $TiAl_3$ on/below the surface of the sintered particle [2,3,6,9,10]. As time progresses all the liquid Al will be consumed and an Al rich intermetallic layer grows and thickens on the sintered particle. Subsequently, Al diffuses inwards and Ti–Al intermetallics evolve in different layers.

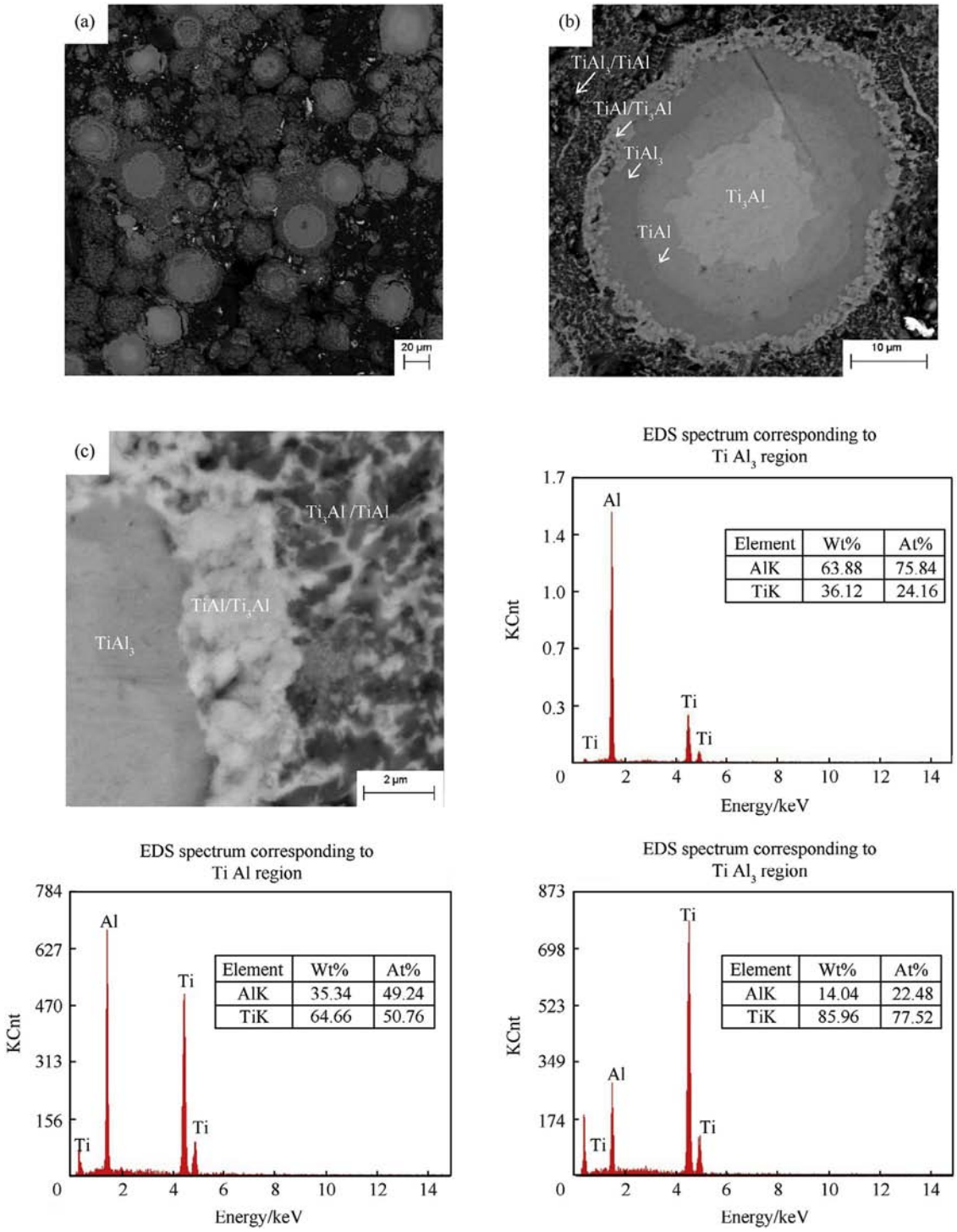

Fig. 3. An SEM (BSE) micrograph of the polished cross-section of a sample sintered at 1000 °C for 6 h. (a) Low magnification micrograph showing overall microstructural features. (b) Individual particle cross-section showing different layers of reaction products. (c) High magnification micrograph showing finer features at the first and second layer interface.

The samples sintered at 1000 °C for 6 h and 24 h also showed similar grainy/globular morphology and the presence of $TiAl_3$ on the particle surfaces. Since the samples sintered at 600 °C and 800 °C were fragile, further microstructural characterization was carried out only on samples sintered at 1000 °C.

Fig. 3 shows the cross-section SEM back scattered electron (BSE) micrograph of the sample sintered at 1000 °C for 6 h. Fig. 3(a) shows a low magnification micrograph indicating particles being fused together by a mixture of $TiAl_3$+TiAl (Fig. 3(c)). Multiple layers, five in total, within the Ti–6Al–4V particle can be clearly observed from Fig. 3(b). The micrograph shows the variation in contrast caused by the composition changes from layer to layer. At least ten EDS spot analyses were performed on each of these layers. The outer periphery consists of a higher percentage of Al with a dark gray background against a white network (Fig. 3(c)), which corresponds to the mixture of $TiAl_3$ (73%–75%Al, 25%–27% Ti by Wt%) and TiAl respectively. The second layer appears as a lighter gray ring, which has the composition of TiAl+Ti_3Al (34%–38%Al, 62%–65%Ti by Wt%). The third layer corresponds to the composition of $TiAl_3$, which is the predominant phase. The fourth layer corresponds to TiAl (48%–50%Al, 48%–52%Ti by Wt%). The inner core has an irregular shape and was identified as Ti_3Al.

Earlier studies on reaction synthesis of TiAl [9–11] from elemental Ti and Al powders were based on the Ti–Al phase diagram, and the sequence of formation of the intermetallics is as follows

$$Ti + Al \rightarrow TiAl_3 \rightarrow TiAl_2 \rightarrow TiAl \rightarrow Ti_3Al$$

Lee et al. synthesized TiAl from elemental powders and also observed multiple layers of intermediate phases in the reacting constituents [10]. However, in the present study, the presence of $TiAl_3$ in the third layer was unexpected according to the Ti–Al phase diagram. This can be explained by the variation in inter-diffusion rates of Ti in Al through the second layer (TiAl+Ti_3Al), and also the sintering time was not sufficient for homogenization of the composition throughout the particle. Mishin and Hertzig reported the inter-diffusion of these elements in TiAl, and concluded that Al diffuses faster than Ti through TiAl [10]. Therefore, enrichment of Al % in the close proximity of TiAl, and simultaneous diffusion of Ti toward the outer surface, results in the formation of $TiAl_3$. Hence, to homogenize the composition and to form TiAl throughout, the samples were sintered for 24 h at 1000 °C. SEM-BSE micrographs of the cross-section of a sample sintered for 24 h are presented in Fig. 4.

Fig. 4(a) shows a typical inter-particle neck region. It can be clearly seen that the bonding region was the result of the overlap of the TiAl+Ti_3Al layers of the individual particles. The original outer periphery, seen in Fig. 3(a), composed of $TiAl_3$, was consumed resulting in the formation of TiAl+Ti_3Al. Fig. 4(b) shows three layers in the particle cross-section micrograph. The outer layer still consists of a very thin layer of $TiAl_3$+TiAl, however, the thickness of the outer layer was lower when compared to the 6 h sintered sample (Fig. 3(c)). The second layer in Fig. 4(b) has a composition of 34%–40%Al and 60%–66%Ti making up TiAl+Ti_3Al. The inner core region corresponds to the composition of intermetallic TiAl (42%–44% Al, 56%–54% Ti). Fig. 4(c) shows a high magnification micrograph of the cross-section of a sintered particle revealing bright isolated, irregular shaped regions. These regions were observed to be enriched with vanadium as indicated by EDS analysis. During

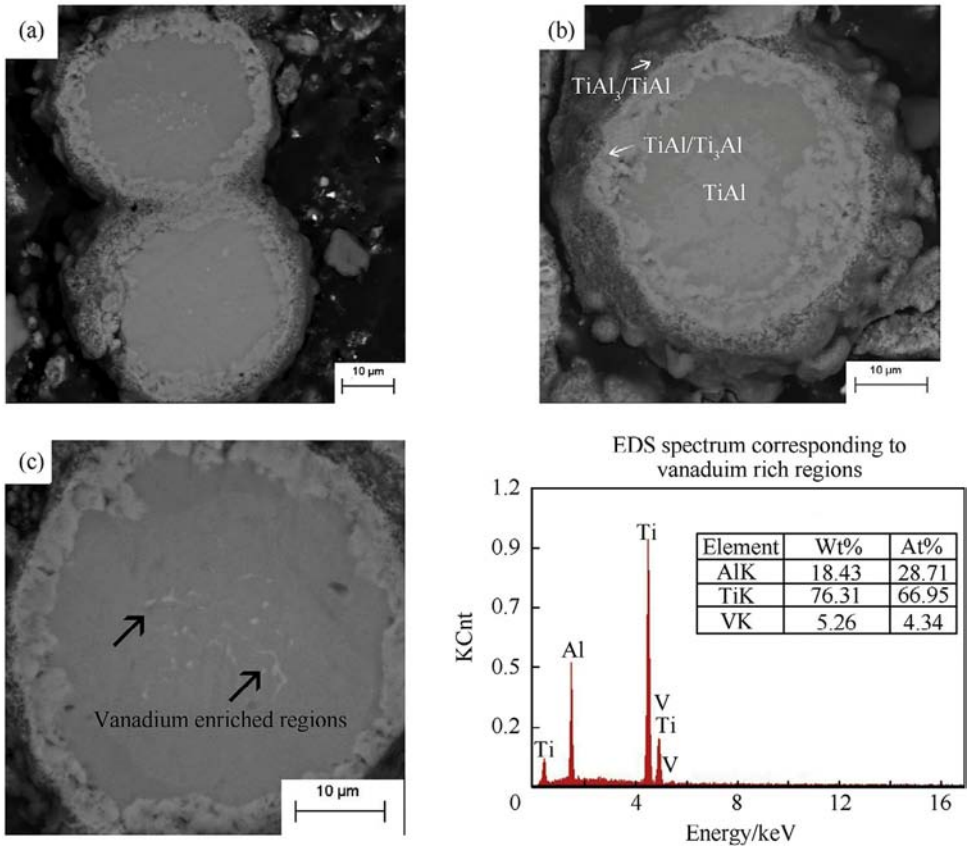

Fig. 4. SEM (BSE) micrograph of the as-polished cross-section of a sample sintered at 1000 °C for 24 h. (a) Region showing the inter-particle bonding region. (b) An individual particle cross-section showing multiple layers.

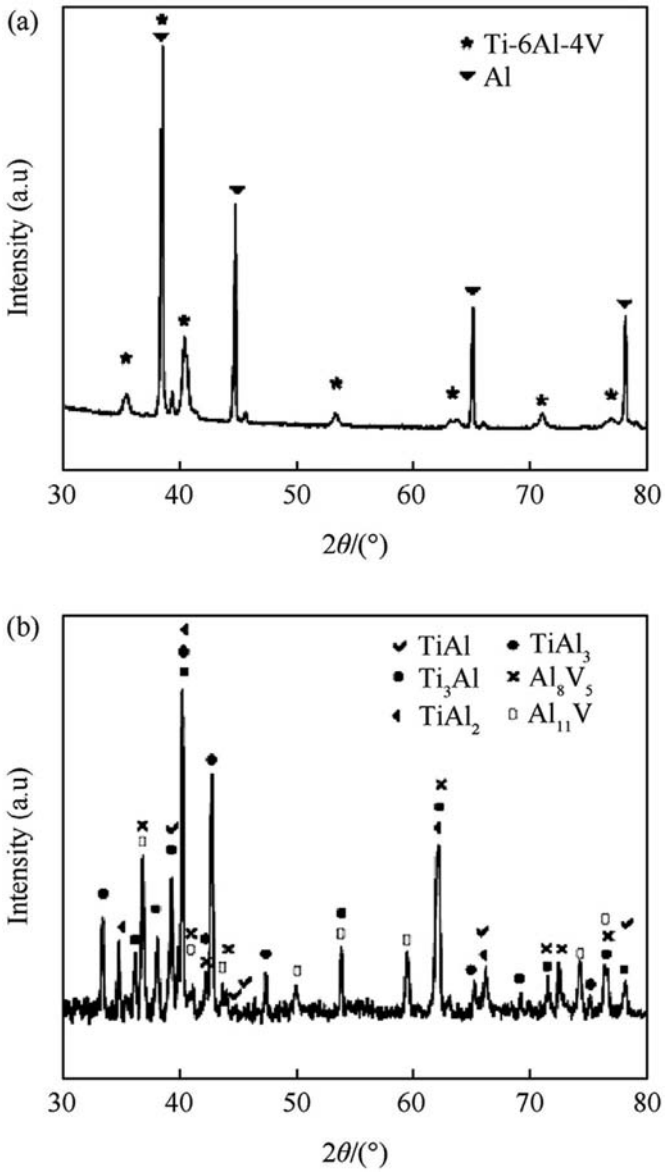

Fig. 5. X-ray diffraction patterns (a) as mixed Ti–6Al–4V powder and Al powder and (b) sample sintered at 1000 °C for 24 h.

reactive sintering and thermal treatment, vanadium present as solid solution in the alloy Ti–6Al–4V was observed to segregate to certain random areas within the sintered particles. This is a consequence of lower solubility of vanadium in the intermetallic phases relative to the high solubility in beta titanium at the sintering temperature. XRD analysis on these samples also reveals the presence of V–Al intermetallic (Fig. 5).

Phase analysis was performed on the as-mixed powders and the sintered sample using X-ray diffraction. An XRD pattern of the powder mixture of Ti–6Al–4V and Al is presented in Fig. 5(a). It can be observed that only elemental Ti and Al peaks were present in the XRD pattern. Fig. 5(b) shows the XRD pattern of the sample sintered at 1000 °C for 24 h. XRD shows the presence of various intermetallic phases formed during reactive sintering. The final microstructure consists of TiAl along with other intermetallic phases such as Al_2Ti, Al_3Ti, $Al_{11}V$, Al_8V_5, and Ti_3Al. The vanadium rich regions correspond to $Al_{11}V$ and/or Al_8V_5 phase in the microstructure shown in Fig. 4(c). The XRD results agree with the SEM analysis of the sintered samples. The density of the part sintered at 1000 °C for 6 h and 24 h was 3.34 g/cm^3 and 3.45 g/cm^3 respectively. Further detailed investigation into the phase evolution, reaction kinetics, and evaluation of mechanical properties is necessary to establish and scale up the process for mass production.

4. Conclusions

This study focused on the fabrication of porous, additive manufactured parts in the TiAl intermetallic alloy. The work reports initial results and evaluates the feasibility of the new approach through the use of a binder jetting process followed by reactive sintering. During high temperature liquid phase sintering Al initially reacts with Ti–6Al–4V particle surfaces and forms Al3Ti. As the sintering time progresses Al diffuses into the Ti–6Al–4V particle and forms TiAl. Microstructural investigation and phase analysis revealed the evolution of a TiAl intermetallic phase along with various other intermediate phases. The present investigation demonstrates that the proposed new approach is capable of producing TiAl intermetallic alloy parts directly from separate Ti–6Al–4V and Al powders using a versatile additive manufacturing method.

References

[1] Welsch G, Boyer R, Collings EW. Materials properties handbook: titanium alloys. Materials Park (OH): ASM International; 1993.
[2] Appel F, Paul JDH, Oehring M. Gamma titanium aluminide alloys: science and technology. John Wiley & Sons; 2011.
[3] Tan P, Tang HP, Kang XT, Wang QB, Zhu JL, Li C, et al. Research on TiAl alloy porous metal flow restrictors. Mater Trans 2009;50(10):2484–7.
[4] Fu-Sheng S, Cao C, Yan M, Kim S, Yong T. Alloying mechanism of beta stabilizers in a TiAl alloy. Metall Mater Trans A 2001;32(7):1573–89.
[5] Loeber L, Biamino S, Ackelid U, Sabbadini S, Epicoco P, Fino P, et al. Comparison of selective laser and electron beam melted titanium aluminides in solid freeform fabrication proceedings. Austin: University of Texas; 2011.
[6] Murr LE, Gaytan SM, Ceylan A, Martinez E, Martinez JL, Hernandez DH, et al. Characterization of titanium aluminide alloy components fabricated by additive manufacturing using electron beam melting. Acta Mater 2010;58:1887–94.
[7] Gibson I, Rosen DW, Stucker B. Additive manufacturing technologies: rapid prototyping to direct digital manufacturing. New York: Springer; 2010.
[8] Miyanaji H, Zhang S, Lassell A, Zandinejad A, Yang L. Process development of porcelain ceramic material with binder jetting process for dental applications. J Miner Met Mater Soc 2016;11:1543–851.
[9] Lee TW, Lee CH. The effect of heating rate on the reactive sintering of Ti-48%Al elemental powder mixture. J Mater Sci Lett 1998;17:1367–70.
[10] Mishin Y, Herzig C. Diffusion in the Ti-Al system. Acta Mater 2000;48:589–623.
[11] Novoselova T, Celotto S, Morgan R, Fox P, O'Neill W. Formation of TiAl intermetallics by heat treatment of cold-sprayed precursor deposits. J Alloys Compd 2007;436:69–77.